Circadian clock control of eIF2α phosphorylation is necessary for rhythmic translation initiation

Shanta Karki[a,b], Kathrina Castillo[a,b], Zhaolan Ding[a,b], Olivia Kerr[a], Teresa M. Lamb[a,b], Cheng Wu[a], Matthew S. Sachs[a], and Deborah Bell-Pedersen[a,b,1]

[a]Department of Biology, Texas A&M University, College Station, TX 77843; and [b]Center for Biological Clocks Research, Texas A&M University, College Station, TX 77843

Edited by Jay C. Dunlap, Geisel School of Medicine at Dartmouth, Hanover, NH, and approved March 31, 2020 (received for review October 22, 2019)

The circadian clock in eukaryotes controls transcriptional and post-transcriptional events, including regulation of the levels and phosphorylation state of translation factors. However, the mechanisms underlying clock control of translation initiation, and the impact of this potential regulation on rhythmic protein synthesis, were not known. We show that inhibitory phosphorylation of eIF2α (P-eIF2α), a conserved translation initiation factor, is clock controlled in *Neurospora crassa*, peaking during the subjective day. Cycling P-eIF2α levels required rhythmic activation of the eIF2α kinase CPC-3 (the homolog of yeast and mammalian GCN2), and rhythmic activation of CPC-3 was abolished under conditions in which the levels of charged tRNAs were altered. Clock-controlled accumulation of P-eIF2α led to reduced translation during the day in vitro and was necessary for the rhythmic synthesis of select proteins in vivo. Finally, loss of rhythmic P-eIF2α levels led to reduced linear growth rates, supporting the idea that partitioning translation to specific times of day provides a growth advantage to the organism. Together, these results reveal a fundamental mechanism by which the clock regulates rhythmic protein production, and provide key insights into how rhythmic translation, cellular energy, stress, and nutrient metabolism are linked through the levels of charged versus uncharged tRNAs.

eIF2α | *cpc-3* | translation initiation | circadian clock | *Neurospora crassa*

Circadian clocks regulate physiology and behavior through the rhythmic control of gene expression to optimize the timing of resource allocation for improved fitness (1). Remarkably, up to 50% of the eukaryotic genome is under control of the clock at the level of rhythmic mRNA abundance (2–8). In addition, mounting evidence supports circadian posttranscriptional regulation, including clock control of mRNA capping, splicing, polyadenylation, and deadenylation (3, 9–14). Rhythmic proteomic analysis in mammalian cells revealed that up to 50% of rhythmic proteins arise from noncycling mRNAs (15–18). Similar results were observed in the well-established circadian model organism *Neurospora crassa* where 41% of the rhythmic proteome arose from arrhythmic mRNAs (18). These data suggested that cycling protein accumulation is driven by temporal protein degradation and/or mRNA translation. In support of clock control of translation, the levels and modification of several translation initiation factors accumulate rhythmically in *N. crassa* (18) and mammals (19, 20), including rhythmic accumulation of translation initiation factor eIF2α levels in mouse liver and brain (21), and cycling phosphorylated eIF2α (P-eIF2α) levels in the mouse suprachiasmatic nucleus (22). Furthermore, the activity of translation elongation factor eEF-2 is controlled by the *N. crassa* clock through rhythmic activation of the p38 MAPK pathway and the downstream eEF-2 kinase RCK-2 (23). However, the mechanisms and extent of clock regulation of translation initiation are not fully understood. Therefore, we investigated the connection between the *N. crassa* clock and translation initiation.

One of the first steps in translation initiation is binding of eIF2 to GTP and the methionyl-initiator tRNA to form the ternary complex (24, 25). The ternary complex associates with the 40S ribosomal subunit to form the 43S preinitiation complex (PIC), which binds to the mRNA cap to form the 48S PIC. The PIC scans the mRNA as an open complex, and upon choosing a start codon in a preferred context, becomes a closed complex with the start codon paired to the initiator tRNA anticodon (26, 27). In the process, eIF2-GDP is released. The 60S ribosomal subunit then joins the 40S subunit to form a functional 80S ribosome for protein synthesis. eIF2-GDP is recycled to eIF2-GTP by the guanine nucleotide exchange factor eIF2B to enable reconstitution of the ternary complex for another round of translation (25).

A central mechanism for translational control is phosphorylation of the α-subunit of eIF2 (25, 28). In mammalian cells, eIF2α can be phosphorylated by four different kinases (GCN2, HRI, PERK, and protein kinase A) in response to different types of extracellular and intracellular stresses (29–31). Among these kinases, GCN2 is conserved in fungi and mammals (32–34). GCN2 is activated by chemical and genetic perturbations that lead to amino acid starvation, and other stresses, which result in the accumulation of uncharged tRNAs (35). Uncharged tRNA binds to the histidyl-tRNA synthetase-like (HisRS) domain and interacts with the C-terminal domain (CTD) of GCN2 to activate the kinase domain (11, 33, 36, 37). In yeast and mammalian cells, GCN1 is required for GCN2 activation (38). GCN1 interacts with ribosomal protein S10 in the ribosomal A site and is thought to transfer uncharged tRNA to activate GCN2 kinase (39, 40). Active GCN2 phosphorylates a conserved serine of eIF2α in fungi and mammals, which inhibits GDP/GTP exchange by

Significance

Circadian clock control of mRNA translation, which contributes to the daily cycling of at least 50% of the proteins synthesized in eukaryotic cells, is understudied. We show that the circadian clock in the model fungus *Neurospora crassa* regulates rhythms in phosphorylation and activity of the conserved translation initiation factor eIF2α, with a peak in phosphorylated eIF2α levels during the daytime. This leads to reduced mRNA translation of select messages during the day and increased translation at night. We demonstrate that rhythmic accumulation of phosphorylated eIF2α requires increased uncharged tRNA levels during the day to activate the eIF2α kinase, coordinating rhythmic translation initiation and protein production with nutrient and energy metabolism.

Author contributions: D.B.-P. designed research; S.K., K.C., Z.D., O.K., T.M.L., and C.W. performed research; S.K., K.C., Z.D., O.K., T.M.L., M.S.S., and D.B.-P. analyzed data; and S.K. and D.B.-P. wrote the paper.

The authors declare no competing interest.

This article is a PNAS Direct Submission.

[1]To whom correspondence may be addressed. Email: dpedersen@bio.tamu.edu.

This article contains supporting information online at https://www.pnas.org/lookup/suppl/doi:10.1073/pnas.1918459117/-/DCSupplemental.

First published April 30, 2020.

eIF2B (28). This reduces translation of many mRNAs, while selectively enhancing the translation of mRNAs that encode proteins required to cope with the stress, including genes encoding key amino acid biosynthetic enzymes (41). Because P-eIF2α is a competitive inhibitor of eIF2B, and because eIF2α is present in excess of eIF2B, small changes in the levels of P-eIF2α in cells are enough to substantially alter protein synthesis (30, 42).

Starvation for all or any single amino acid, as well as too much of any one amino acid, leads to an amino acid imbalance, alterations in the levels of charged tRNAs, activation of GCN2, and synthesis of all 20 amino acids to relieve the imbalance (43–46). This general amino acid control (30), originally called cross-pathway control in *N. crassa* (46), leads to the activation of GCN2 kinase, phosphorylation of eIF2α, and translation of the bZIP transcription factors CPC-1 in *N. crassa*, and Gcn4 in yeast (30, 32). Both *cpc-1* and GCN4 contain upstream open reading frame (uORF) in the 5′ mRNA leader sequence that control translation of the main ORF in response to amino acid imbalance and the accumulation of P-eIF2α (30, 47–49).

The critical role for eIF2α in cap-dependent translation initiation led us to examine if, and how, the *N. crassa* circadian clock regulates translation initiation by regulating the phosphorylation state and activity of eIF2α. We show that ∼30% of available *N. crassa* eIF2α is phosphorylated during the subjective day under control of the circadian clock. CPC-3 rhythmic activity, which was altered by chemical and/or genetic perturbation of amino acid levels and the levels of uncharged tRNA, was necessary for rhythmic accumulation of P-eIF2α. This daytime peak in P-eIF2α levels corresponded with increased levels of uncharged tRNA during the day, and to reduced translation in cell-free translation assays prepared from those cells. Furthermore, while the core clock component FREQUENCY (FRQ) accumulated rhythmically in Δ*cpc-3* cells, indicating the circadian oscillator was not impacted by P-eIF2α levels, we confirmed that one gene whose expression was predicted to be controlled at the level of translation by P-eIF2α levels, ALG-11, had protein rhythms that were dependent on CPC-3 and rhythmic P-eIF2α levels in vivo. These data suggested that clock regulation of P-eIF2α levels by CPC-3 drives rhythmic translation of specific mRNAs, rather than controlling global rhythmic translation, uncovering potential clock control of select mRNA translation by conserved mechanisms.

Results

eIF2α Phosphorylation Is Clock Controlled. To determine whether the *N. crassa* circadian clock regulates translation initiation, rhythms in phosphorylation of eIF2α (NCU08277) were investigated. Protein extracts were isolated from *N. crassa* cells grown in constant dark (DD) over a 2-d circadian time course. The protein extracts were used to assay the levels of total and P-eIF2α with anti-mammalian eIF2α antibodies directed against conserved epitopes (Fig. 1 and *SI Appendix*, Fig. S1*A*). eIF2α is essential; therefore, the specificity of the antibodies could not be confirmed using a deletion of eIF2α. Instead, antibody directed against total eIF2α was confirmed to cross-react with *N. crassa* eIF2α expressed and purified from bacteria with a band corresponding to the appropriate molecular weight (36 kDa) (*SI Appendix*, Fig. S1*B*). The specificity of the phosphospecific eIF2α antibody (P-eIF2α antibody) was confirmed by the signal being dependent on CPC-3 kinase (NCU01187) (Fig. 2*A*), and by stimulation of the signal during histidine starvation using 3-amino-1,2,4-triazole (3-AT) treatment (50) (see Fig. 4*A*).

In wild-type (WT) cells, P-eIF2α levels (Fig. 1*A* and *SI Appendix*, Fig. S1*C*), but not total eIF2α levels (Fig. 1*B* and *SI Appendix*, Fig. S1*D*), cycled with a daily rhythm, reaching peak levels in the subjective late morning (DD16 and DD40). The levels of P-eIF2α and total eIF2α fluctuated in clock mutant Δ*frq* cells, but rhythmicity of P-eIF2α accumulation was abolished (Fig. 1*C*). These data demonstrated that the rhythm in P-eIF2α accumulation is controlled by the circadian clock.

CPC-3 Is Required for Phosphorylation of eIF2α. To determine whether CPC-3 kinase is required for phosphorylation of eIF2α in *N. crassa*, the levels and phosphorylation status of eIF2α were examined in Δ*cpc-3* cells grown in a circadian time course in DD (Fig. 2). No P-eIF2α was detected in Δ*cpc-3* cells in DD (Fig. 2*A*), whereas eIF2α was detected at all time points (Fig. 2*B*). Furthermore, complementation of Δ*cpc-3* cells with a WT copy of *cpc-3* rescued P-eIF2α to a level similar to that observed in WT cells in DD (Fig. 2*C*). These data supported that CPC-3 kinase is necessary for eIF2α phosphorylation when cells are grown in DD.

Because eIF2α is a general translation initiation factor that may be critical for expression of components of the molecular circadian oscillator, we examined whether Δ*cpc-3* cells retain a functional clock by assaying canonical FRQ protein rhythms (51) from the same extracts used to examine P-eIF2α levels (Fig. 2*A*). FRQ protein levels were rhythmic in both WT and Δ*cpc-3* cells (Fig. 2*D* and *SI Appendix*, Fig. S1*E*). In addition, Δ*cpc-3* had no significant effect on the period of the circadian rhythm of development in strains carrying the *ras-1*^{bd} mutation (Fig. 2*E*), which slows growth rate and clarifies the rhythm in asexual spore development (52). However, the linear growth rate in *ras-1*^{bd}, Δ*cpc-3* was slower compared to *ras-1*^{bd} cells. The growth rate of Δ*cpc-3* was also slower than WT cells grown in DD (Fig. 4*C*). Thus, CPC-3 is necessary for phosphorylation of eIF2α, and for normal linear growth rate in DD. However, neither CPC-3 nor rhythmic P-eIF2α levels are required for a functional circadian oscillator.

Rhythmic Phosphorylation of eIF2α Is Not Dependent on Rhythmic CPC-3 Levels. Phosphorylation of eIF2α is rhythmic and requires CPC-3 in DD. Rhythmic control of eIF2α phosphorylation might be due to clock control of the levels and/or activity of CPC-3 kinase. To first establish whether the clock controls the levels of *cpc-3* mRNA and protein, WT and Δ*frq* cells were transformed with either a *cpc-3* promoter::luciferase transcriptional fusion (*Pcpc-3::luc*), or a CPC-3::V5 translational fusion. *Pcpc-3::luc* and CPC-3::V5 accumulated rhythmically in WT, but not in Δ*frq*, cells grown in DD (Fig. 3 *A* and *B* and *SI Appendix*, Fig. S2 *A* and *B*). The peak in CPC-3::V5 levels occurred during the subjective day (DD12–DD16 and DD40), similar to the peak in P-eIF2α levels (Fig. 1*A*), and consistent with the data from a proteomics study demonstrating that CPC-3 protein levels cycled under control of the clock (18). Clock control of CPC-3 protein levels supported the possibility that rhythmic accumulation of CPC-3 is necessary for rhythmic P-eIF2α accumulation. To test this possibility, CPC-3 was constitutively expressed from a copper regulatable *Ptcu-1* promoter (53), and in the presence of *Ptcu-1* inducer bathocuproinedisulfonic acid (BCS), constitutive expression of CPC-3::V5 protein was observed over a circadian time course (Fig. 3*C* and *SI Appendix*, Fig. S2*C*). However, constitutive expression of CPC-3 protein did not alter rhythmic P-eIF2α levels (Fig. 3*D* and *SI Appendix*, Fig. S2*D*). These data indicated that rhythmic accumulation of CPC-3 protein is not sufficient to explain the rhythms in P-eIF2α levels. Instead, these data raised the possibility that the activity of CPC-3 is clock controlled, and that it is the control of CPC-3 activity, not levels, that accounts for the rhythm in P-eIF2α levels.

Constitutive Activation of CPC-3 Abolished Rhythmic P-eIF2α Levels. In *Saccharomyces cerevisiae*, GCN2 kinase is activated upon binding of uncharged tRNA to the regulatory domains (33, 36, 37). In addition, activation of GCN2 by uncharged tRNA requires the transacting positive effector protein GCN1 (54). The regulatory domains of *S. cerevisiae* GCN2 are conserved in *N.*

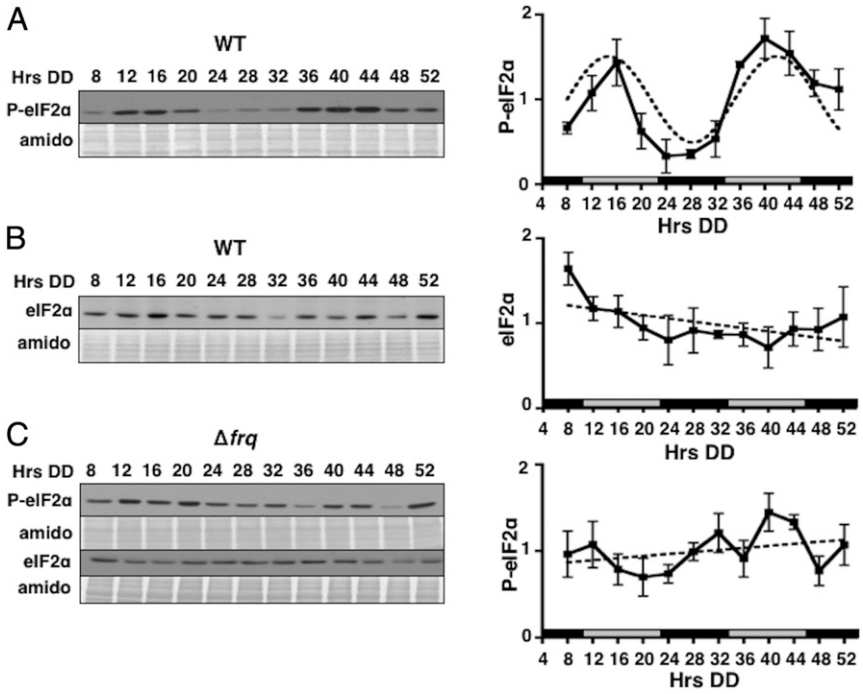

Fig. 1. The circadian clock regulates the activity of eIF2α. Representative Western blots of protein extracts isolated from WT (*A* and *B*) or Δ*frq* (*C*) strains grown in a circadian time course and probed with anti–P-eIF2α antibody (*A* and *C*) or total eIF2α antibody (*B* and *C*). The same protein extracts were used in *A* and *B*. Amido black-stained protein is shown as a loading control. Plots of the data (mean ± SEM; $n = 3$) on the *Right* show the average P-eIF2α (*A* and *C*) or eIF2α (*B*) signal normalized to total protein (solid black line). Rhythmicity of P-eIF2α in WT cells (*A*) was determined using *F* tests of fit of the data to a sine wave (dotted black line; $P < 0.001$), while eIF2α in WT cells (*B*), and both eIF2α and P-eIF2α in Δ*frq* cells (*C*) were arrhythmic as indicated by a better fit of the data to a line (dotted black lines). The black and white bars at the *Bottom* of the plots designate subjective day (gray) and night (black) in this and all subsequent figures. See *SI Appendix*, Fig. S1 for the full gels in WT cells. The Western blots were done separately; therefore, the levels of P-eIF2α (*A* and *C*) and eIF2α (*B* and *C*) are not comparable between WT and Δ*frq* cells (see Fig. 6*A* for a comparison of P-eIF2α levels in WT and Δ*frq* cells).

crassa CPC-3 (34); therefore, we hypothesized that CPC-3 is similarly activated by uncharged tRNA and GCN1 (NCU05803). To first establish whether CPC-3 is activated by amino acid starvation, 3-AT, a competitive inhibitor of imidazoleglycerol-phosphate dehydratase enzyme necessary for histidine production (55), was added to *N. crassa* cultures 8 h prior to harvest at the peak (DD40) and trough (DD28) of P-eIF2α levels (Fig. 1*A*). As a result of clock control, the levels of P-eIF2α were twofold higher in untreated WT cells at DD40 compared to DD28 (Fig. 4*A*). However, in 3-AT–treated cells, the time-of-day difference in P-eIF2α levels was abolished, and the overall levels of P-eIF2α were approximately threefold higher than the peak at DD40 in WT cells. As expected, no significant change in total eIF2α levels was observed in 3-AT–treated versus untreated cells at either time point. These data demonstrated that up to 30% of eIF2α is phosphorylated by the clock during the day (DD40) compared to maximum levels of P-eIF2α during amino acid starvation. Consistent with the requirement for binding of uncharged tRNA for activation, CPC-3 required GCN1 for activation of the kinase domain to phosphorylate eIF2α, but deletion of GCN1 had no effect on total eIF2α levels (Fig. 4*B* and *SI Appendix*, Fig. S3*A*), or on FRQ::LUC protein rhythms (*SI Appendix*, Fig. S3*B*). However, compared to WT cells, the linear growth rate of Δ*gcn-1* was reduced to a level comparable to Δ*cpc-3* cells (Fig. 4*C*). These data are consistent with the idea that, similar to *S. cerevisiae* GCN2, *N. crassa* CPC-3 requires uncharged tRNA and GCN1 for activation. Therefore, we predicted that the corresponding mutations known to constitutively activate GCN2 in *S. cerevisiae* would constitutively activate *N. crassa* CPC-3, and provide the tool needed to examine whether rhythmic CPC-3 activity is required for cycling P-eIF2α levels.

In *S. cerevisiae*, the F835L mutation leads to constitutive activation of GCN2, independent of uncharged tRNA binding, dimerization, association with ribosomes, and association with GCN1 (56). The homologous mutation generated in *N. crassa* CPC-3, *cpc-3*^{c}, led to a greater than threefold increase in P-eIF2α levels but had no significant effect on total eIF2α levels compared to WT cells grown for 28 h in DD (Fig. 4*D*). To validate that the *cpc-3*^{c} mutation bypasses the requirement for activation by binding of uncharged tRNA, we showed that P-eIF2α levels were similar to WT levels in Δ*gcn1; cpc-3*^{c} cells (Fig. 4*B*). These data supported that, in *cpc-3*^{c} mutant cells, CPC-3 is constitutively active, and this activity is independent of the requirement for GCN1 and uncharged tRNA.

Next, to determine whether P-eIF2α rhythmicity requires rhythmic activation of CPC-3, we examined P-eIF2α levels in *cpc-3*^{c} strains in a circadian time course in DD. If clock control of the activity of CPC-3 is necessary for rhythmic P-eIF2α accumulation, then the levels of P-eIF2α should be high and arrhythmic in *cpc-3*^{c} cells. Indeed, in the *cpc-3*^{c} mutant, the levels of P-eIF2α were higher compared to WT (Fig. 4*D*) and arrhythmic (Fig. 4*E*), with no corresponding change in the levels of total eIF2α (Fig. 4*D* and *SI Appendix*, Fig. S3*C*). Furthermore, the clock functioned normally in the mutant, as demonstrated by robust FRQ::LUC protein rhythms in *cpc-3*^{c} cells (*SI Appendix*, Fig. S3*B*). Similar to the reduced growth in Δ*cpc-3* and Δ*gcn1* that lack P-eIF2α accumulation, constitutive activation of CPC-3, and the resulting high and arrhythmic accumulation of P-eIF2α, also led to a reduction in linear growth rate compared to WT cells (Fig. 4*C*). Thus, CPC-3 activity is regulated by the clock, and this regulation is necessary for the rhythmic accumulation of P-eIF2α and normal linear growth rate.

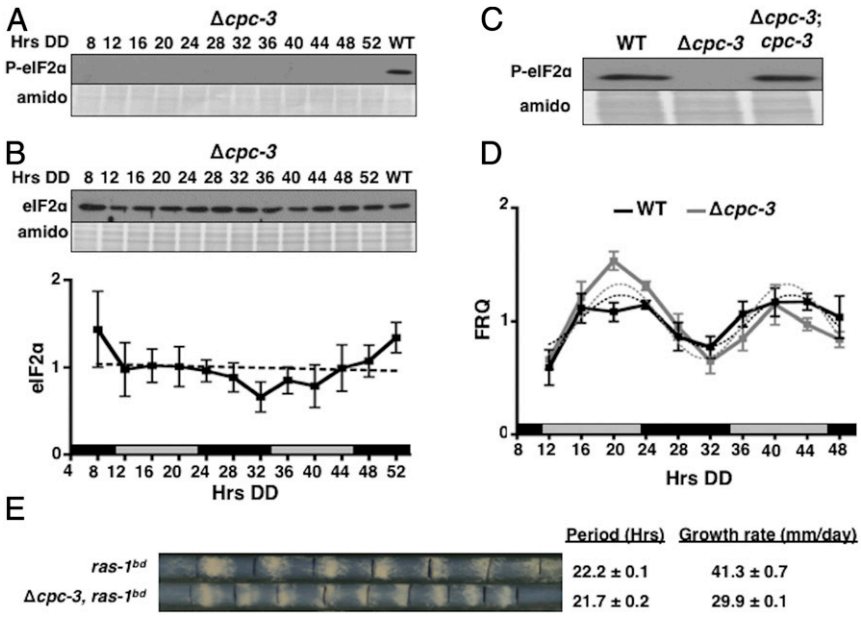

Fig. 2. CPC-3 is required for phosphorylation of eIF2α and normal linear growth rate, but not for a functional clock. (*A*) Western blot of protein extracted from Δ*cpc-3* cells grown in a circadian time course and probed with anti–P-eIF2α antibody (*A*), or total eIF2α antibody (*B*). The data in *B* are plotted below. Total eIF2α levels were arrhythmic as determined using *F* tests of fit of the data to a line (dotted black line). (*C*) Western blot of protein extracted from WT, Δ*cpc-3* and Δ*cpc-3* complemented cells (Δ*cpc-3; cpc-3*) grown in DD for 40 h and probed with anti–P-eIF2α antibody. Amido-stained protein is shown as loading controls in *A*–*C*. (*D*) FRQ protein was analyzed by Western blot in WT and Δ*cpc-3* cells (*SI Appendix*, Fig. S1*E*), and FRQ protein levels are plotted. FRQ rhythmicity in both strains was determined using *F* tests of fit of the data to a sine wave (dotted lines; $P < 0.001$). (*E*) Race tube assay of the indicated strains. Period and linear growth rates of the strains are indicated on the *Right* (mean ± SD; $n = 15$).

Clock control of CPC-3 activity could be through rhythms in uncharged tRNA levels, and/or GCN1 levels. To test these ideas, we first examined whether GCN1 protein levels cycle by generating a GCN1::LUC translational fusion. The levels of GCN1::LUC cycled in WT cells, peaking in the early subjective night (*SI Appendix*, Fig. S4*A*). The observed nighttime peak in GCN1:LUC levels would not

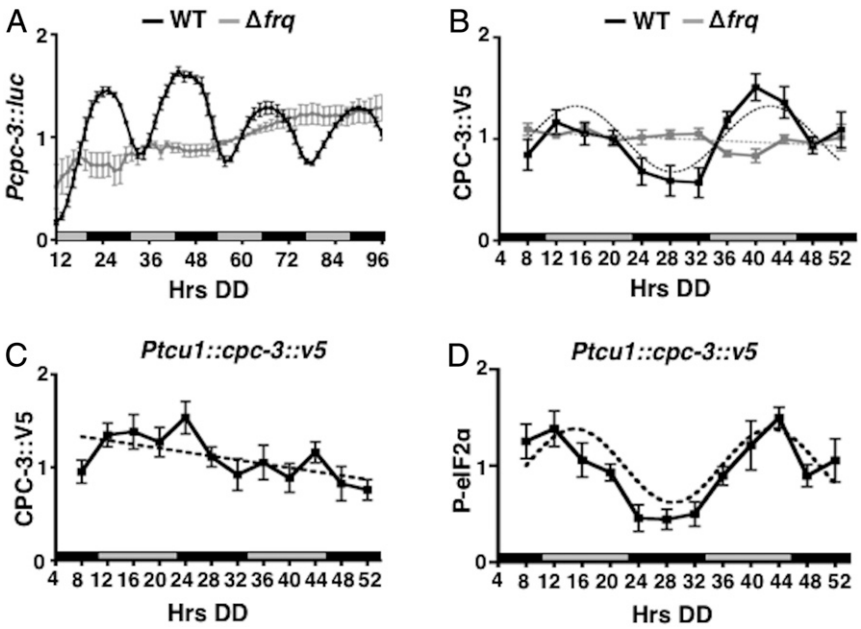

Fig. 3. The rhythmic abundance of CPC-3 is not required for rhythmic P-eIF2α levels. (*A*) Bioluminescence measurements from a *Pcpc-3::luc* transcriptional fusion construct expressed in WT (black line) or Δ*frq* (gray line) cells and recorded in DD every 90 min over 4 d (Hrs DD) ($n = 10$). (*B*) Plot of CPC-3::V5 protein levels from WT and Δ*frq* cells grown in a circadian time course. See *SI Appendix*, Fig. S2 *A* and *B* for the Western blots. Rhythmicity of CPC-3::V5 cells in WT was determined using *F* tests of fit of the data to a sine wave ($P < 0.001$), whereas CPC-3::V5 levels in Δ*frq* cells was better fit to a line (dotted lines). Plot of CPC-3::V5 (*C*) and P-eIF2α (*D*) protein levels from *Ptcu1::cpc-3::v5* cells grown in a circadian time course with BCS. See *SI Appendix*, Fig. S2 *C* and *D* for the Western blots. CPC-3::V5 levels were best fit to a line (*C*, black dotted line), and P-eIF2α to a sine wave (*D*, black dotted line; $P < 0.005$).

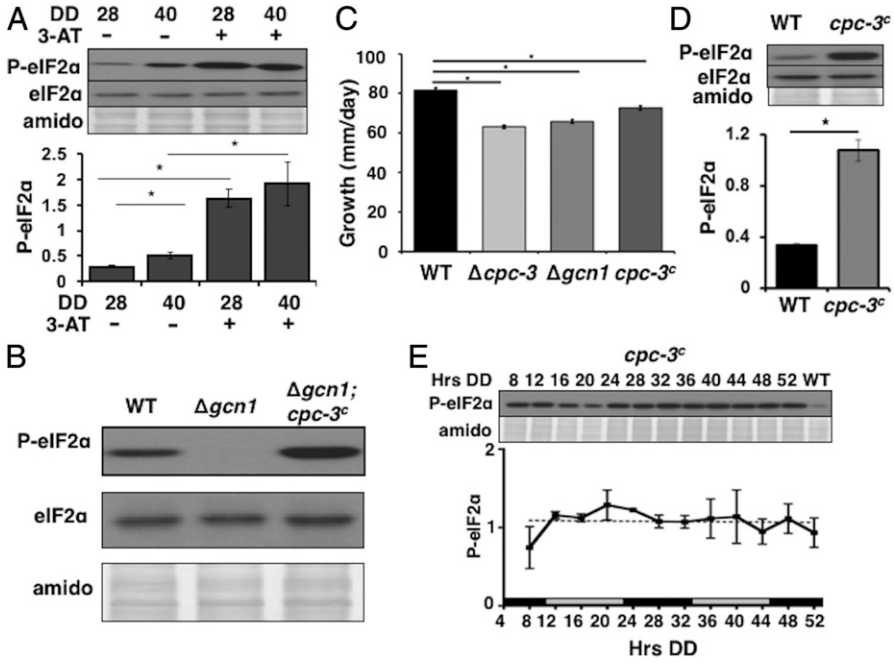

Fig. 4. Rhythmic activation of CPC-3 is required for rhythmic phosphorylation of eIF2α. (*A*) Western blots of protein from WT cells treated (+) or not (–) with 3-AT and harvested in the subjective day (DD40) or night (DD28). The data are plotted below. (*B*) Western blot of protein from the indicated cells harvested in the subjective day (DD28). The blots were probed with anti–P-eIF2α antibody or total eIF2α antibody. Amido black-stained protein is shown below as a loading control. (*C*) Linear growth (millimeters per day) was determined for the indicated strains cultured on race tubes in DD. The data are plotted (mean ± SEM; $n = 9$; $^*P < 0.01$). (*D*) Western blot of protein from the indicated cells harvested in the subjective day (DD28) and probed with anti–P-eIF2α antibody or total eIF2α antibody. Amido black-stained protein is shown below as a loading control. The data are plotted below. The graphs in *A* and *D* show the average signal normalized to total protein loaded (mean ± SEM; $n = 3$; $^*P < 0.004$, Student *t* test). (*E*) Western blot of protein isolated from *cpc-3*^{c} cells grown in a circadian time course, and including a WT sample harvested at DD40, and probed with anti–P-eIF2α antibody. The data are plotted below (mean ± SEM; $n = 3$). P-eIF2α levels were arrhythmic as indicated by a better fit of the data to a line (dotted black lines).

be expected if GCN1 directly controlled rhythmic CPC-3 activity, given that CPC-3 activity peaks during the subjective day. However, to rule out the possibility that the daytime accumulation of GCN1 might be sufficient for rhythmic CPC-3 activity, GCN1 was tagged with the HA epitope, and GCN1::HA was constitutively expressed from *Ptcu-1* (53). In the presence of the *Ptcu-1* inducer BCS, GCN1::HA levels were arrhythmic (*SI Appendix*, Fig. S4*B*), but the loss of rhythmic accumulation GCN1::HA had no effect on cycling P-eIF2α levels (*SI Appendix*, Fig. S4*C*). Therefore, while these data cannot rule out clock control of the activity of GCN1, we suspected that rhythms in the levels of uncharged tRNA accounts for rhythmic activation of CPC-3 during the subjective day.

Rhythms in uncharged tRNA levels could arise from rhythms in amino acid levels or aminoacyl-tRNA synthetase (aaRS) levels. Metabolic analysis of free amino acid levels in *N. crassa* WT cells did not reveal a significant rhythm for any of the 19 amino acids detected under our growth conditions (*SI Appendix*, Fig. S5), despite reported circadian rhythms in amino acid biosynthetic enzymes and their corresponding mRNAs (2, 18, 57). However, several aaRSs, including valyl-tRNA synthetase (ValRS) (NCU01965), were reported to cycle in abundance at the mRNA and/or protein levels (18, 57), which could lead to a rhythm in the balance of uncharged versus charged tRNAs. A translational fusion of ValRS to LUC (ValRS::LUC) confirmed that ValRS protein levels are rhythmic in WT, but not in clock mutant Δ*frq* cells, with a peak in the subjective night (*SI Appendix*, Fig. S6*A*). We predicted that the trough in ValRS during the subjective day would lead to increased levels of uncharged $tRNA^{Val}$ and activation of CPC-3 during the subjective day. To first test this prediction, P-eIF2α levels were assayed in the temperature-sensitive ValRS mutant *un-3*^{ts}, which leads to an ∼50% reduction in ValRS activity when cells are grown at the permissive temperature (25 °C) (58). Consistent with a role for uncharged tRNA in activating CPC-3, the levels of P-eIF2α were high and arrhythmic in the *un-3*^{ts} mutant over a circadian time course (Fig. 5*A*), whereas FRQ protein level cycling was unaffected in the mutant (Fig. 5*B* and *SI Appendix*, Fig. S6*B*). Complementation of *un-3*^{ts} with a WT copy of *valRS* rescued P-eIF2α rhythmicity (*SI Appendix*, Fig. S6*C*). Next, the levels of uncharged ValRS were measured over a circadian time course. The levels of uncharged ValRS cycled with a low amplitude, with a peak during the subjective day in WT cells (Fig. 5*C*), but were arrhythmic in clock mutant Δ*frq* (Fig. 5*D*) and *un-3*^{ts} (*SI Appendix*, Fig. S6*D*) cells. The levels of total $tRNA^{val}$ did not cycle (*SI Appendix*, Fig. S6*E*). Together, these data supported that circadian rhythms in the ratio of charged versus uncharged tRNAs drive rhythmic CPC-3 activity, which in turn directs the daytime peak in P-eIF2α levels.

Clock Control of P-eIF2α Activity Is Required for Rhythmic Translation of Select Transcripts In Vitro and In Vivo. Phosphorylation of eIF2α leads to an overall decrease in protein synthesis (28), and the clock regulates rhythms in the levels of P-eIF2α in *N. crassa*. Thus, we predicted that translation of some mRNAs would be reduced during the subjective day when the levels of P-eIF2α are high, and that translation would be increased during the subjective night when the levels of P-eIF2α are low. As an initial test of this prediction, we carried out in vitro translation assays using cell-free extracts isolated from WT, Δ*frq*, and Δ*cpc-3* cells harvested at the peak (DD40) and trough (DD28) of rhythmic P-eIF2α levels, that were programmed with capped polyadenylated mRNA encoding firefly luciferase (LUC). Translation was monitored by quantitating LUC activity (Fig. 6*A*). As predicted, LUC translation was higher when P-eIF2α levels were

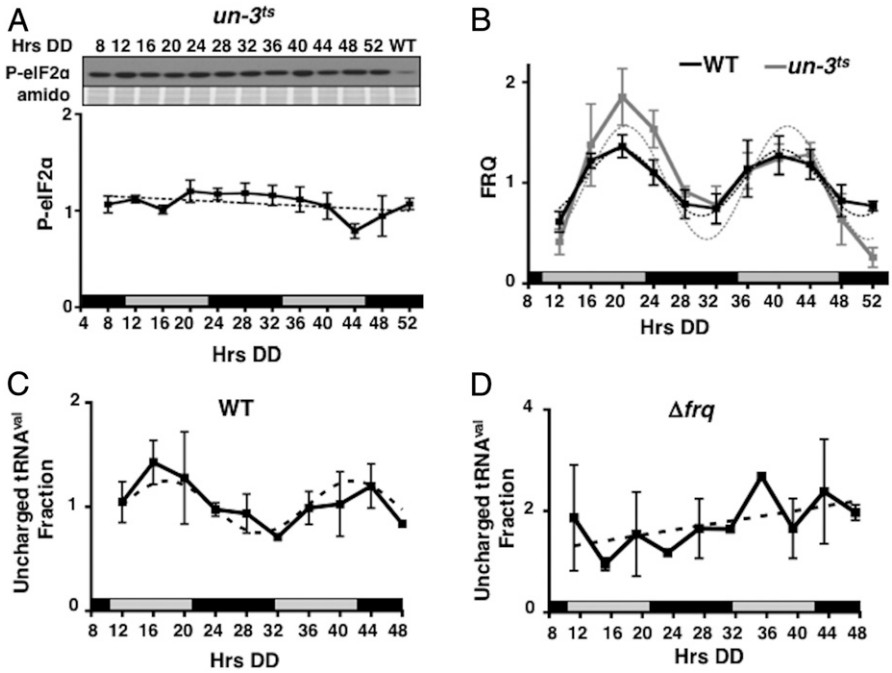

Fig. 5. Rhythms in uncharged tRNA levels are necessary for rhythmic CPC-3 activity and P-eIF2α accumulation. (*A*) Western blot of P-eIF2α levels in the *un-3*^{ts} mutant grown in a circadian time course and harvested at the indicated times (Hrs DD). A WT sample harvested at DD28 is shown to demonstrate high levels of P-eIF2α in the mutant, and amido-stained protein is shown below as a loading control. The data are plotted below (mean ± SEM; $n = 3$). P-eIF2α levels were arrhythmic as indicated by a better fit of the data to a line (dotted black line). (*B*) FRQ protein was analyzed by Western blot in WT and *un-3*^{ts} mutant cells over a circadian time course (*SI Appendix*, Fig. S6*B*), and FRQ protein levels are plotted (mean ± SEM; $n = 3$). FRQ rhythmicity in both strains was determined using *F* tests of fit of the data to a sine wave (dotted lines; $P < 0.001$). Plot of the levels of uncharged tRNA^{val} over a circadian time course in (*C*) WT (mean ± SEM; $n = 3$) and (*D*) Δ*frq* cells (mean ± SEM; $n = 2$). The data for WT was fit to a sine wave (dotted lines; $P < 0.001$), whereas the data for Δ*frq* was fit to a line.

low during the subjective evening (DD28), and translation was reduced at the peak of P-eIF2α levels in the subjective day (DD40). In Δ*frq* cells, LUC translation was similar to WT DD28 at both times of the day, supporting that the clock is necessary for increased P-eIF2α during the day. In Δ*cpc-3* extracts, LUC translation was significantly higher at both times of day, reflecting the absence of P-eIF2α under these growth conditions (Fig. 2). These data supported that clock control of the levels of P-eIF2α provides a mechanism to regulate rhythmic translation initiation.

To investigate a role for rhythmic P-eIF2α accumulation on mRNA translation in vivo, we examined rhythmicity of *alg-11* (NCU06779) mRNA and ALG-11 protein levels in WT, Δ*frq*, and Δ*cpc-3* cells. ALG-11, a mannosyl transferase involved in N-linked glycosylation of proteins, was chosen based on its conserved role in posttranslational modifications important in cell wall stability, signaling, and endoplasmic reticulum protein quality control (59). In addition, our preliminary RNA-seq and ribosome profiling data showed that while *alg-11* mRNA levels are arrhythmic, the clock controls rhythms in ribosome occupancy on *alg-11* mRNA. These data suggested that *alg-11*, which contains a uORF (*SI Appendix*, Fig. S7), is regulated at the translational level by the clock. In WT cells, an ALG-11::LUC translational reporter fusion was rhythmic in DD, peaking during subjective night when P-eIF2α levels are low, whereas an *alg-11* promoter *luc* fusion (P*alg-11::luc*, a transcriptional reporter) was arrhythmic (Fig. 6*B*). Consistent with translation regulation by the clock and rhythmic eIF2α activity, ALG-11::LUC was arrhythmic in Δ*frq* and Δ*cpc-3* cells (Fig. 6 *C* and *D*), as well as in *un-3*^{ts} cells (*SI Appendix*, Fig. S7*C*). These data demonstrated that ALG-11 protein rhythms, which arise from constant mRNA levels, require a functional clock and rhythmic eIF2α activity.

Discussion

Translation initiation is a tightly regulated process that requires several translation initiation factors. One of the main targets of translational control is eIF2α. We established that the *N. crassa* clock regulates the activity of eIF2α (Fig. 1), with inhibitory P-eIF2α levels peaking during the subjective day and active eIF2α levels peaking during the subjective night. The nighttime activity of eIF2α parallels the peak activity of eEF-2 (23), suggesting coordinate control of mRNA translation initiation and elongation at night.

Consistent with the idea of coordinate circadian control of initiation and elongation, translation peaked at night in vitro when P-eIF2α (Fig. 6*A*) and PeEF-2 (23) levels are low. Similarly, the level of ALG-11 protein expression, which requires CPC-3 for rhythmic mRNA translation, peaked at night (Fig. 6*B*). In independent studies, mass spectroscopy analyses of rhythmic protein accumulation in *N. crassa* revealed that about 27% of the identified proteome accumulated with a circadian rhythm, with an approximately twofold increase in rhythmic protein accumulation at night compared to the day (2). In contrast, the peak in rhythmic mRNA levels was biphasic, with most transcripts peaking during the late night to early morning (2, 18, 57, 60).

Interestingly, *N. crassa* clock-controlled genes involved in catabolism generally peak during the day to provide energy for anabolic functions that occur at night (2, 57). As protein synthesis is energetically costly, it makes sense for the organism to synchronize most translation to the night when energy resources are at their maximum to support growth. Indeed, disruption of rhythmic P-eIF2α levels in *N. crassa* led to a significant reduction in linear growth rate (Fig. 4*C*). Conversely, some proteins accumulate to high levels during the day under control of the clock (18). A daytime peak in protein levels may be, in part, due to only up to one-half of available eIF2α and eEF-2 reaching peak

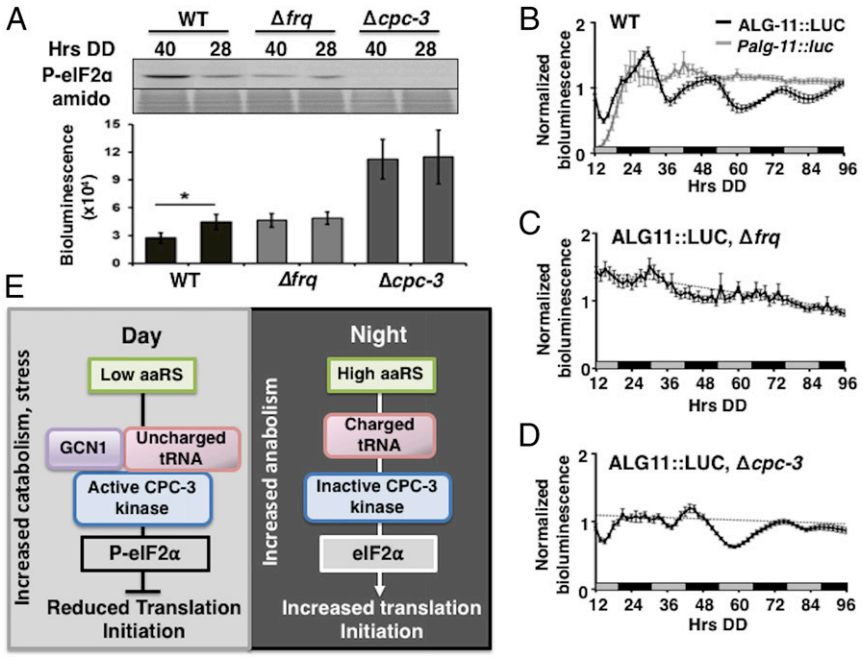

Fig. 6. Clock control of P-eIF2α levels is required for rhythmic translation in vitro and in vivo. (*A*) In vitro translation of *luc* mRNA using *N. crassa* cell-free extracts from WT, Δ*frq*, and Δ*cpc-3* cells harvested in the subjective day (DD40) or night (DD28). Western blots (*Top*) of the indicated strains were probed with anti–P-eIF2α antibody. Amido-stained protein is shown below as a loading control. The plot below shows the average bioluminescence signal from translation of *luc* mRNA (*$P < 0.05$; $n = 3$). (*B*) Luciferase activity from ALG-11::LUC translational (black line) and *Palg-11::luc* transcriptional (gray line) fusions in WT cells, and (*C*) ALG-11::LUC in Δ*frq* and (*D*) Δ*cpc-3* cells grown in DD and recorded every 90 min over 4 d (Hrs DD). The average bioluminescence signal is plotted (mean ± SEM; $n = 12$). ALG-11::LUC in Δ*frq* and Δ*cpc-3* cells was arrhythmic as indicated by a better fit of the data to a line (dotted black lines). (*E*) Model of how the circadian clock regulates of mRNA translation through daytime activation of CPC-3. See *Discussion* for details of the model.

phosphorylation levels under control of the clock in constant environmental conditions (Fig. 4*A* and ref. 23), allowing some mRNAs to escape the daytime inhibition of translation. Moreover, phosphorylation of eIF2α selectively enhances translation of some target mRNAs, particularly those with uORFs in the leader sequence (49, 61, 62). Similar situations are observed in mice, in which some neuronal mRNAs involved in memory processing have increased translation when eEF-2 is hyperphosphorylated (63), and in *Aplysia* neurons, where eEF-2 phosphorylation promotes the translation of some messages, while repressing others (64). Taken together, these data support that certain mRNAs are more sensitive to increased daytime P-eIF2α and P-eEF-2 levels, and therefore peak in translation at night when energy levels are predicted to be high, whereas others are less sensitive, or are specifically activated, and peak in levels during the day, possibly to deal with predictable increases in environmental stress during the daylight hours. However, acute stress at any time of the day overrides circadian regulation of eEF-2 activity (23), and eIF2α activity as demonstrated by constitutive phosphorylation of eIF2α in the presence of 3-AT (Fig. 4*A*).

While P-eIF2α rhythms are necessary for the rhythmic accumulation of ALG-11 (Fig. 6), they are not required for rhythmic FRQ protein accumulation and a functional clock (Fig. 2 *D* and *E*), supporting that some, but not all, rhythmic proteins are derived from rhythmic translation. However, the full impact of clock-control of eIF2a activity on translation across the genome, and the mechanisms underlying whether or not an mRNA is sensitive to increased P-eIF2α levels during the subjective day, are not yet known. Interestingly, FRQ (65) and ALG-11 (*SI Appendix*, Fig. S7) mRNAs contain uORFs. While uORFs have been associated with increased translation when P-eIF2α levels are high (30, 49, 62), their presence alone in mRNAs would not be sufficient to predict regulation by rhythmic P-eIF2α levels. Although our data show that rhythmic P-eIF2α does not significantly alter the core clock mechanism in *N. crassa*, a recent study of the mammalian circadian clock found that a similar daytime peak in levels of P-eIF2α in the suprachiasmatic nucleus (SCN) promoted the translation of *Atf4*, which in turn, activated transcription of the core clock gene *Per2* (22). As a result, mutations or drugs that decreased P-eIF2α levels in the SCN lengthened circadian period, whereas mutations or drugs that increased P-eIF2α levels shortened the period. Despite differences in the effect of rhythmic P-eIF2α on the clock between *N. crassa* and mice, these data demonstrate a significant and conserved role for the regulation of translation initiation through eIF2α activity by the clock and its impact on the physiology of the organism.

Rhythmic CPC-3 activity (Fig. 4*E*), but not cycling CPC-3 levels (Fig. 3 *C* and *D*), is necessary for the daytime peak in P-eIF2α levels. Activation of GCN2 requires binding of uncharged tRNA to the HisRS domain and the CTD, leading to a conformational change, activation of GCN2 protein kinase domain, and phosphorylation of eIF2α (25, 36, 37, 66). Because the HisRS domain is conserved in all GCN2 homologs (37), we speculated that CPC-3 in *N. crassa* is similarly activated by rhythmic binding of uncharged tRNA. Consistent with this idea, histidine starvation, induced by the addition of 3-AT to *N. crassa* cells, abolished the time-of-day difference in P-eIF2α levels (Fig. 4*A*). Amino acid levels accumulate rhythmically in the mouse brain under control of the clock (67), and in *N. crassa*, genes involved in amino acid biosynthesis are clock controlled (2, 18, 57). However, we did not observe a rhythm in free amino acid levels when *N. crassa* cells were cultured in DD. Alternatively, several aaRS mRNAs and proteins were reported in genome-wide studies to be clock controlled (2, 18, 57), and we validated that ValRS protein levels are rhythmic, peaking at night (*SI Appendix*, Fig. S6*A*). We found that reduced activity of ValRS led to high and arrhythmic P-eIF2α levels (Fig. 5*A*). In addition,

3-AT treatment of *N. crassa* cells results in inhibition of His-tRNA charging (68), and consistent with a role for uncharged tRNAs in CPC-3 activity, we showed that P-eIF2α levels were high and arrhythmic in cells treated with 3-AT (Fig. 4*A*). Furthermore, we discovered that uncharged $tRNA^{val}$ levels, but not total levels of $tRNA^{val}$, cycle under control of the clock with a peak during the subjective day, corresponding to daytime activation of CPC-3 (Fig. 5 *C* and *D* and *SI Appendix*, Fig. S6*E*). Although surprisingly little is known about the regulation of aaRS genes, these data suggest that the levels of aaRSs are rate limiting. This might be expected given that the K_m of aaRSs for their respective amino acids are typically low, in the micromolar range, whereas the amount of free amino acids are typically in molar concentrations (69). While starvation for amino acids (e.g., through exposure to chemical inhibitors, or through mutation) induces CPC3/GCN2 activity, modulating cellular amino acid levels to the extent needed to achieve a change in availability required to affect tRNA charging for circadian regulation would be more difficult than limiting the activity of the aaRSs themselves. Taken together, our data support that a change in the levels or activity of an aaRS, such as what occurs on a daily basis under control of the circadian clock, has systemwide consequences for tRNA charging and activation of CPC-3. Future experiments will focus on determining the mechanisms of clock control of the aaRS genes. Last, in *S. cerevisiae*, protein phosphatases Sit4 and Glc7 remove the phosphate from P-eIF2α (70, 71). We are currently testing whether the homologous phosphatases in *N. crassa* are active at night to remove the phosphate from P-eIF2α to augment nighttime translation initiation.

Based on these and published data, our current working model is that increased uncharged tRNA levels during the subjective day, resulting from clock control of aaRS genes, and their delivery by GCN1 to CPC-3 lead to activation of CPC-3, increased P-eIF2α levels, and reduced translation initiation (Fig. 6*E*). In addition, decreased charging of tRNAs would be expected to slow translation elongation rates in the context of high P-eEF-2 levels. As a result, during the day, mRNA translation would be generally low, and protein catabolism would rise. Nighttime peaks in aaRSs would lead to increased charged tRNA levels, low CPC-3 activity and inhibitory P-eIF2α levels, and enhanced mRNA translation at night. While our data cannot rule out the possibility that rhythmic GCN1 activity might be required for cycling CPC-3 activity, the finding that CPC-3 and GCN1 levels cycle, but that rhythmic accumulation is not necessary for the daytime peak in CPC-3 activity and P-eIF2α levels, suggest that cycling CPC-3 and GCN1 levels may have additional functions in the cell and/or increase the robustness of CPC-3 activity rhythms.

Reprogramming protein production through CPC-3/GCN2 activity provides a conserved mechanism for organisms to quickly adapt to significant changes in the levels of amino acids, energy, and the ratio of charged versus uncharged tRNAs, such as during acute nutrient deprivation. Control of the activity of initiation and elongation factors and their kinases by the clock under normal physiological conditions adds a further level of regulation to allow integration of nighttime anabolic and daytime catabolic cellular pathways with protein translation to effectively utilize available energy resources, and to contend with predictable daily stress.

Materials and Methods

***N. crassa* Strains and Growth Conditions.** A list of strains, key reagents, and oligonucleotides are listed in *SI Appendix*, Table S1. Vegetative growth conditions and crossing protocols were as previously described (72). All strains containing the *hph* construct were maintained on Vogel's minimal media (72), supplemented with 200 μg/mL hygromycin B. Strains containing the *bar* cassette were maintained on Vogel's minimal media lacking NH_4NO_3 and supplemented with 0.5% proline and 200 μg/mL Basta. Race tube assays to monitor developmental rhythms in strains carrying the *ras-1^{bd}* mutation, and linear growth rates, were accomplished using 1× Vogels salt, 0.1% glucose, 0.17% arginine, and 50 μg/mL biotin media as previously described (53).

To assay *cpc-3* mRNA rhythms, a *Pcpc-3::luc* transcriptional fusion was generated by first amplifying a 1.5-kb promoter fragment upstream of the *cpc-3* coding region using primers LUCF1 and LUCR1 containing NotI and AscI restriction sites. The resulting 1.5-kb fragment was cloned into pRMP57 containing an *N. crassa* codon-optimized luciferase gene (26), linearized with NdeI, and transformed into WT cells (Fungal Genetics Stock Center #4200 [FGSC#4200]), and transformants were assayed for luciferase activity. *Pcpc-3::luc* transformants were crossed with WT (FGSC#2489) and *Δfrq::bar* (DBP1228) strains to generate *Pcpc-3::luc* (DBP2439) and *Pcpc-3::luc*, *Δfrq::bar* (DBP2442) homokaryons.

A GCN1::LUC translational fusion was generated by three-way PCR with 1.5 kb of *gcn1* (73) ORF (gcn1 F1 and R1 primers), 1.65 kb of *N. crassa* codon-optimized luciferase gene (gcn1 F2 and R2 primers), 1.0 kb of 3′ *gcn1* (gcn1 F3 and R3), and cotransformed into WT cells (FGSC#4200) with plasmid for pBARGEM7-2 (74) for Basta selection. The *gcn1* gene was targeted for replacement by the GCN1::LUC construct via homologous recombination. Basta-resistant transformants were picked, screened for luciferase activity, and endogenous integration of GCN1::LUC was validated using *gcn1* F4, R4, F5, and R5 primers.

cpc-3::v5::hph was generated by three-way PCR with 1.4 kb of the *cpc-3* ORF (primers V5F1 and V5R1), 1.8 kb 10× glycine linker-V5-hygromycin-B resistance gene (*hph*) (primers V5F2 and V5R2), and 1 kb of the 3′ end of *cpc-3* (primers VF3 and V5R3). PCR was used to verify endogenous integration of the construct into the *cpc-3* locus using V5F4 and V5R4 primers, and expression of CPC-3::V5 was validated by Western blot using anti-V5 antibody. A *cpc-3::v5::hph* homokaryon (DBP2717) was generated by transforming WT with *cpc-3::v5::hph*, followed by crossing with WT (FGSC#2489). For overexpression of CPC-3::V5, a *bar::P_{tcu-1}::cpc-3::v5::hph* strain was generated by transforming a three-way PCR product containing 1.5 kb of the 5′ *cpc-3* ORF (primers tcu1F1 and tcuR1), *bar::P_{tcu-1}* from plasmid DBP450 (primers tcu1F2 and tcuR2) (53), and 1 kb of 3′ end of *cpc-3* (primers tcu1F3 and tcuR3) into the DBP2717 strain. Following validation of integration by PCR (primers tcu1F4 and tcuR4), a *bar::P_{tcu-1}::cpc-3::v5::hph* homokaryon (DBP2742) was obtained by microconidia filtration (75).

For overexpression of GCN-1::HA from the *tcu-1* promoter, 5′ and 3′ integrating fragments of DNA, consisting of 5′ flank *gcn1::3′bar* (primers gcn1^{OE}F1 and barR), and 5′*bar::P_{tcu-1}::gcn1* ORF (primers barF and gcn1^{OE}R3), respectively, were transformed into WT cells (FGSC#4200), creating DBP3473. Colonies were selected on 250 μg/mL glufosinate ammonium, and proper integration was confirmed by PCR using primers gcn1^{OE}-validF and gcn1^{OE}-validR.

A GCN1::HA translational fusion was created by three-way PCR with 1.8 kb of the *gcn1* ORF (primers gcn1-F1 and gcn1-R1), 0.183 kb of 3× glycine linker-HA (primers gcn1-F2 and gcn1-R2), and 2.1 kb (primers gcn1::HA-F3 and gcn1::HA-R3) of the 3′ flank of *gcn1*. The GCN1::HA construct was cotransformed into DBP3473 with hyg^R plasmid pCSR1::hph (76). Transformants were selected on plates containing hygromycin B and were validated for endogenous integration using gcn1::HA-validF and HA-validR. GCN1::HA expression was confirmed by Western blotting using anti-HA primary antibody. A ValRS::LUC translational fusion was generated by three-way PCR (valRSF1 and valRSR1, and valRSF3 and valRSR3 primers) using the *N. crassa* codon-optimized luciferase gene from pRMP57 (primers valRSF2 and valRSR3) (26, 73), and cotransformed with hyg^R pBP15 (77) into WT (FGSC#4200) cells. Hygromycin-resistant transformants were screened for luciferase activity and homologous insertion into the *valRS* gene (primers valRSF4 and valRSR4).

To generate the constitutive active *cpc-3^c* mutation, phenylalanine at codon 835 (TTC) and serine 837 (TCT) of CPC-3 was changed to leucine (CTG), and serine (TCT), respectively, to create a BclI restriction enzyme site. The mutant 3.8-kb fragment was generated by two-way PCR using primers *cpc-3^c* F1, *cpc-3^c*R1, *cpc-3^c*F2, and *cpc-3^c*R2, verified by sequencing, and then cotransformed with the hyg^R pBP15 plasmid (77) into *Δmus-52::bar* (FGSC#9719). A transformant containing *cpc-3^c* was crossed to WT (FGSC#4200) and *Δgcn1* (FGSC#14201) to obtain DBP3290 (*cpc-3^c*) and DBP3292 (*Δgcn1; cpc-3^c*) homokaryons, respectively. Progeny from the crosses were screened by PCR using primers *cpc-3^c*F3 and *cpc-3^c*R3, followed by restriction digestion with BclI.

The ALG-11::LUC translational fusion was generated by three-way PCR (alg-11F2 and alg-11R2, and alg-11F4 and alg-11R4 primers) using the *N. crassa* codon-optimized luciferase gene from pRMP57 (primers alg-11F3 and alg-11R3) (26, 73), and cotransformed with either hyg^R pBP15 (77) into WT (FGSC#2489), *Δfrq* (DBP1320), and *un-3^{ts}* (FGSC#81) strains, or with BASTA^R

pBARGEM7-2 (74) into Δ*cpc-3* cells (FGSC#10697). Hygromycin or Basta-resistant transformants were screened for luciferase activity and homologous insertion into the *alg-11* gene (primers alg-11F5 and alg-11R5).

To generate the P*alg-11::luc* transcriptional fusion, a 1.3-kb promoter region of *alg-11* was amplified with primers alg-11F1 and alg-11R1 containing XmaI restriction sites. The PCR product was digested with XmaI and cloned into plasmid pRMP57 containing the codon-optimized luciferase gene (73). The resulting plasmid was linearized by digestion with PciI, cotransformed with hyg^R pBP15 (77) into WT (FGSC2489) cells, and hygromycin-resistant transformants were screened for luciferase activity.

To assay FRQ::LUC protein rhythms, strains FGSC#14201, FGSC#10697, or DPB3290, were crossed to strains containing a FRQ::LUC translational fusion linked to *bar* (78). Hygromycin and Basta-resistant progeny were screened for luciferase activity to generate *frq::luc*, *Δgcn1* (DBP3321), *frq::luc*, *Δcpc-3* (DBP2789), and *frq::luc, cpc-3^c* (DBP3315) strains. *cpc-3^c* was validated by PCR using cpc-3^{c}F3 and cpc-3^{c}R3 primers followed by restriction digestion with BclI.

Circadian Time Courses. Circadian time course experiments for Western blots and amino acid analyses were accomplished according to published methods (79) as follows. Mycelial mats in Vogel's minimal media containing 2% glucose (pH 6.0) were synchronized to the same time of day by a shift from 30 °C light (LL) to 25 °C dark (DD). The cultures were grown in LL for a minimum of 4 h and transferred to DD on day 1 (for collection at DD36, -40, -44, -48, -52), day 2 (for collection at DD12, -16, -20, -24, -28, -32), day 3 (for collection at DD8), and harvested either at 9:00 AM (DD12, -16, -20, -36, -40, -44) or 5:00 PM (DD8, -24, -28, -32, -48, -52) on day 3. Harvested tissue was immediately frozen in liquid N_2. For constitutive expression of *bar::P$_{tcu\text{-}1}$::cpc-3::v5::hph*, cells were grown in Vogel's medium containing 30 μM of the copper chelator BCS to induce the *tcu-1* promoter (53).

Complementation of Δ*cpc-3* and *un-3^{ts}*. Complementation of Δ*cpc-3* was done to validate that CPC-3 was required for P-eIF2α rhythms. A WT copy of *cpc-3* was amplified from the genome by PCR (primers cpc-3F1and cpc-3R1) using Phusion Hot Start High-Fidelity DNA polymerase. The primer pair amplified 1.5 kb upstream of the *cpc-3* coding region, the 5.8 kb *cpc-3* ORF, and 1 kb downstream of the *cpc-3* coding region. The PCR product was cotransformed with a Basta-resistant plasmid pBARGEM7-2 (74) into Δ*cpc-3* (FGSC#10697). Transformants were selected for Basta resistance and validated for having a WT copy of *cpc-3* by PCR using primers cpc-3F2 and cpc-3R2. Complementation of *un-3^{ts}* was done to validate that valRS was required for P-eIF2α rhythms. A WT copy of *valRS* was amplified from WT genomic DNA by PCR (primers un3compF1 and un3compR1) using Phusion High-Fidelity DNA polymerase. The primer pair amplified 1.2 kb upstream of the *valRS* coding region, the 5.9-kb *cpc-3* ORF, and 1.4 kb downstream of the *valRS* coding region. The construct was cotransformed with hyg^R pBP15 (77) into the *un-3^{ts}* strain (FGSC#81). Hygromycin-resistant transformants were selected and validated for having a WT copy of *valRS* by growth at 30 °C and for rhythmic P-eIF2α levels.

3-AT Treatment. To determine whether CPC-3 is activated by amino acid starvation, germinating conidia were treated with 3-AT. Conidia (1×10^5) from WT and Δ*cpc-3* strains were inoculated in 500 mL of Vogel's minimal media containing 2% glucose. Conidia were germinated in LL at 25 °C for 4 h, and then transferred to DD at 25 °C. A final concentration of 9 mM 3-AT was added to the cultures 8 h before harvesting at the indicated time points for Western blotting.

Protein Extraction and Western Blotting. Protein was extracted as previously described (80) with the following modification: the extraction buffer contained 100 mM Tris pH 7.0, 1% SDS, 10 mM NaF, 1 mM PMSF, 1 mM sodium ortho-vanadate, 1 mM β-glycerophosphate, 1× aprotinin, 1× leupeptin hemisulfate salt, and 1× pepstatin A. Protein concentration was determined by the Bradford assay. Protein samples (50 μg) were separated on 8% SDS/PAGE gels and blotted to an Immobilon-P nitrocellulose membrane according to standard methods.

The levels of P-eIF2α were detected using rabbit monoclonal anti-EIF2S1 antibody diluted 1:5,000 in 5% BSA, 1× TBS, 0.1% Tween, and anti-rabbit IgG HRP secondary antibody diluted 1:10,000. Total eIF2α levels were detected using rabbit polyclonal anti-EIF2S1 antibody diluted 1:5,000, and anti-rabbit IgG HRP secondary antibody diluted 1:10,000. CPC-3::V5 was detected using mouse monoclonal anti-V5 antibody diluted 1:5,000 in 5% milk, 1× TBST, 0.1% Tween, and anti-mouse IgG HRP secondary antibody diluted 1:10,000. FRQ protein was detected using mouse monoclonal anti-FRQ antibody diluted 1:200 in 7.5% milk, 1× TBS, 0.1% Tween, and anti-mouse IgG-HRP secondary antibody diluted at 1:10,000. All proteins except FRQ were detected using chemiluminescence SuperSignal West Pico Substrate. FRQ was detected using SuperSignal West Femto Maximum Sensitivity Substrate. Densitometry was performed using NIH ImageJ software (81) and normalized to protein loading using amido black-stained protein.

Purification of eIF2α. To validate the specificity of total eIF2α antibody, eIF2α was first amplified from *N. crassa* cDNA with primers eIF2F1 and eIF2R1 containing restriction sites for NdeI and NotI. The PCR product and pET30b vector were digested with NdeI and NotI prior to ligation to create pDBP607, which creates an IPTG inducible eIF2α-6His fusion plasmid for expression in *Escherichia coli*. pDBP607 was transformed to *E. coli* BL21 cells and transformed cells were grown at 37 °C overnight in 5 mL of Luria broth (LB), supplemented with 30 μg/mL kanamycin for selection. For purification of eIF2α, 1 mL of the overnight culture was inoculated into 50 mL of LB at 37 °C with shaking at 250 rpm until an OD of 0.63 was reached. A final concentration of 1 mM IPTG was added to induce expression, and cells were chilled and harvested 3 h after IPTG addition. Total eIF2α was purified by batch binding of a guanidinium buffer lysate to a Ni-NTA column and eluting with denaturing elution buffer according to published methods (82). After purification, the protein was dialyzed against multiple volumes of 10 mM Tris-Cl, pH 8.0, 0.1% Triton X-100, and then brought up to a final concentration of 20 ng/μL in 10% glycerol, 100 mM NaCl, and 0.1 mM EDTA. Purified protein was visualized by Western blot using total eIF2α antibody.

Luciferase Assays. To examine bioluminescence rhythms arising from strains containing luciferase fusions, 1×10^5 conidia were inoculated into 96-well microtiter plates containing 150 μL of 1× Vogel's salts, 0.01% glucose, 0.03% arginine, 0.1 M quinic acid, 1.5% agar, and 25 μM firefly luciferin, pH 6. After inoculation of conidia (1×10^5 conidia), the microtiter plate was incubated at 30 °C in LL for 24 h and transferred to DD at 25 °C to obtain bioluminescence recordings using EnVision Xcite Multilabel Reader, with recordings taken every 90 min over 4 to 5 d. Raw luciferase activity data were analyzed for period, phase, and amplitude using BioDARE (83). Raw reads were normalized to the mean to graph the data.

Amino Acid Analysis. Free amino acid levels were measured in WT and Δ*frq* cells over a circadian time course in Vogel's 2% glucose medium. Cells were washed with cold water and harvested using vacuum filtration, followed by flash freezing in liquid nitrogen. Frozen tissue was crushed into a thin powder using a mortar and pestle. Crushed cells (0.35 g) were boiled in 600 μL of distilled water for 20 min, followed by centrifugation for 15 min at 14,000 rpm. Supernatant (500 μL) was transferred to a VIVASPIN 500 column concentrator with a molecular weight cutoff of 5,000 Da, followed by centrifugation at 4° for 45 min at 14,000 rpm. The samples were analyzed for free amino acid levels by HPLC in the Protein Chemistry Lab Core Facility, Texas A&M University. Ten microliters of the sample were used for amino acid quantification.

In Vitro Translation. In vitro translation of *luc* mRNA was accomplished as previously described (23, 84).

tRNA Charging Assay. To examine rhythms in the levels of $tRNA^{val}$, a tRNA charging assay was performed (85). Total RNA was extracted from ground tissue obtained from circadian time courses of WT (FGSC#4200) and *un-3^{ts}* (FGSC#81) strains. The pH was maintained at 4.5 throughout the RNA isolation to prevent deacylation. Two micrograms of RNA was treated with 12.5 mM $NaIO_4$ or 12.5 mM NaCl in sodium acetate buffer (pH 4.5) in the dark for 20 min, and then quenched with 0.25 M glucose for 10 min at 25 °C. Each sample was spiked with 7.3 ng of deacylated yeast $tRNA^{phe}$ and processed using MicroSpin G-25 columns to remove the salt. Desalted RNA was subjected to deacylation by resuspension in 50 mM Tris·HCl (pH 9.0), incubation at 37 °C for 45 min, followed by precipitation with cold 100% ethanol. Four hundred nanograms of tRNA was ligated to a 5′-adenylated linker (primer tRNAqPCR-linker) using T4 RNA ligase 2 truncated. An oligo (primer tRNAqPCR-GSP) complementary to the linker was used to generate cDNA with SuperScript RT III First-Strand Synthesis System. cDNA was diluted 1:10 and used as a template for quantitative PCR to detect val-specific tRNA using the corresponding primer pairs: yeast $tRNA^{phe}$ (primers sc-$tRNA^{phe}$-F and sc-$tRNA^{phe}$-R) and *N. crassa* $tRNA^{val}$ (primers nc-$tRNA^{val}$-F and sc-$tRNA^{val}$-R). The data were normalized to yeast $tRNA^{phe}$, and the uncharged $tRNA^{val}$ fraction was calculated by subtracting the charged fraction ($NaIO_4$-treated) from total $tRNA^{val}$ (NaCl-treated).

Statistical Analysis. Rhythmic data were fit to a sine wave or a line as previously described (79). Nonlinear regression to fit the rhythmic data to a sine wave (fitting period, phase, and amplitude) and a line (fitting slope and intercept), as well as Akaike's information criteria tests to compare the fit of each dataset to the two equations, were carried out using the Prism software package. The *P* values reflect the probability that, for instance, the sine wave fits the data better than a straight line. The Student *t* test was used to determine significance in changes in the levels of P-eIF2α when compared between DD28 and DD40, and after induction with 3-AT. Error bars in all graphs represent the SEM from at least three independent experiments, unless otherwise indicated.

Materials and Data Availability. All strains generated in the study are available upon request until they are deposited at the Fungal Genetics Stock Center (FGSC), http://www.fgsc.net/. All data are made available in the paper.

ACKNOWLEDGMENTS. This work was funded by NIH Grants R01 GM058529 and R35 GM126966 to D.B.-P.

1. V. K. Sharma, Adaptive significance of circadian clocks. *Chronobiol. Int.* **20**, 901–919 (2003).
2. J. M. Hurley *et al*., Analysis of clock-regulated genes in *Neurospora* reveals widespread posttranscriptional control of metabolic potential. *Proc. Natl. Acad. Sci. U.S.A.* **111**, 16995–17002 (2014).
3. N. Koike *et al*., Transcriptional architecture and chromatin landscape of the core circadian clock in mammals. *Science* **338**, 349–354 (2012).
4. J. S. Menet, J. Rodriguez, K. C. Abruzzi, M. Rosbash, Nascent-seq reveals novel features of mouse circadian transcriptional regulation. *eLife* **1**, e00011 (2012).
5. C. L. Partch, C. B. Green, J. S. Takahashi, Molecular architecture of the mammalian circadian clock. *Trends Cell Biol.* **24**, 90–99 (2014).
6. M. W. Vitalini, R. M. de Paula, W. D. Park, D. Bell-Pedersen, The rhythms of life: Circadian output pathways in *Neurospora*. *J. Biol. Rhythms* **21**, 432–444 (2006).
7. C. Vollmers *et al*., Circadian oscillations of protein-coding and regulatory RNAs in a highly dynamic mammalian liver epigenome. *Cell Metab.* **16**, 833–845 (2012).
8. R. Zhang, N. F. Lahens, H. I. Ballance, M. E. Hughes, J. B. Hogenesch, A circadian gene expression atlas in mammals: Implications for biology and medicine. *Proc. Natl. Acad. Sci. U.S.A.* **111**, 16219–16224 (2014).
9. J. M. Fustin *et al*., RNA-methylation-dependent RNA processing controls the speed of the circadian clock. *Cell* **155**, 793–806 (2013).
10. V. Bélanger, N. Picard, N. Cermakian, The circadian regulation of Presenilin-2 gene expression. *Chronobiol. Int.* **23**, 747–766 (2006).
11. J. E. Baggs, C. B. Green, Nocturnin, a deadenylase in *Xenopus laevis* retina: A mechanism for posttranscriptional control of circadian-related mRNA. *Curr. Biol.* **13**, 189–198 (2003).
12. J. O. Lipton *et al*., The circadian protein BMAL1 regulates translation in response to S6K1-mediated phosphorylation. *Cell* **161**, 1138–1151 (2015).
13. M. Zhou *et al*., Non-optimal codon usage affects expression, structure and function of clock protein FRQ. *Nature* **495**, 111–115 (2013).
14. Y. Xu *et al*., Non-optimal codon usage is a mechanism to achieve circadian clock conditionality. *Nature* **495**, 116–120 (2013).
15. M. S. Robles, J. Cox, M. Mann, In-vivo quantitative proteomics reveals a key contribution of post-transcriptional mechanisms to the circadian regulation of liver metabolism. *PLoS Genet.* **10**, e1004047 (2014).
16. D. Mauvoisin *et al*., Circadian clock-dependent and -independent rhythmic proteomes implement distinct diurnal functions in mouse liver. *Proc. Natl. Acad. Sci. U.S.A.* **111**, 167–172 (2014).
17. A. B. Reddy *et al*., Circadian orchestration of the hepatic proteome. *Curr. Biol.* **16**, 1107–1115 (2006).
18. J. M. Hurley *et al*., Circadian proteomic analysis uncovers mechanisms of post-transcriptional regulation in metabolic pathways. *Cell Syst.* **7**, 613–626.e5 (2018).
19. C. Jouffe *et al*., The circadian clock coordinates ribosome biogenesis. *PLoS Biol.* **11**, e1001455 (2013).
20. R. Cao *et al*., Translational control of entrainment and synchrony of the suprachiasmatic circadian clock by mTOR/4E-BP1 signaling. *Neuron* **79**, 712–724 (2013).
21. R. Wang, X. Jiang, P. Bao, M. Qin, J. Xu, Circadian control of stress granules by oscillating EIF2α. *Cell Death Dis.* **10**, 215 (2019).
22. S. S. Pathak *et al*., The eIF2alpha kinase GCN2 modulates period and rhythmicity of the circadian clock by translational control of Atf4. *Neuron* **104**, 724–735.e6 (2019).
23. S. Z. Caster, K. Castillo, M. S. Sachs, D. Bell-Pedersen, Circadian clock regulation of mRNA translation through eukaryotic elongation factor eEF-2. *Proc. Natl. Acad. Sci. U.S.A.* **113**, 9605–9610 (2016).
24. T. E. Dever, R. Green, The elongation, termination, and recycling phases of translation in eukaryotes. *Cold Spring Harb. Perspect. Biol.* **4**, a013706 (2012).
25. A. G. Hinnebusch, J. R. Lorsch, The mechanism of eukaryotic translation initiation: New insights and challenges. *Cold Spring Harb. Perspect. Biol.* **4**, a011544 (2012).
26. J. Wei, Y. Zhang, I. P. Ivanov, M. S. Sachs, The stringency of start codon selection in the filamentous fungus *Neurospora crassa*. *J. Biol. Chem.* **288**, 9549–9562 (2013).
27. A. G. Hinnebusch, Structural insights into the mechanism of scanning and start codon recognition in eukaryotic translation initiation. *Trends Biochem. Sci.* **42**, 589–611 (2017).
28. N. Sonenberg, A. G. Hinnebusch, Regulation of translation initiation in eukaryotes: Mechanisms and biological targets. *Cell* **136**, 731–745 (2009).
29. M. Dey *et al*., Mechanistic link between PKR dimerization, autophosphorylation, and eIF2alpha substrate recognition. *Cell* **122**, 901–913 (2005).
30. A. G. Hinnebusch, Translational regulation of GCN4 and the general amino acid control of yeast. *Annu. Rev. Microbiol.* **59**, 407–450 (2005).
31. A. P. Han *et al*., Heme-regulated eIF2alpha kinase (HRI) is required for translational regulation and survival of erythroid precursors in iron deficiency. *EMBO J.* **20**, 6909–6918 (2001).
32. P. Zhang *et al*., The GCN2 eIF2alpha kinase is required for adaptation to amino acid deprivation in mice. *Mol. Cell. Biol.* **22**, 6681–6688 (2002).
33. A. Gárriz *et al*., A network of hydrophobic residues impeding helix alphaC rotation maintains latency of kinase Gcn2, which phosphorylates the alpha subunit of translation initiation factor 2. *Mol. Cell. Biol.* **29**, 1592–1607 (2009).
34. E. Sattlegger, A. G. Hinnebusch, I. B. Barthelmess, *cpc-3*, the *Neurospora crassa* homologue of yeast GCN2, encodes a polypeptide with juxtaposed eIF2alpha kinase and histidyl-tRNA synthetase-related domains required for general amino acid control. *J. Biol. Chem.* **273**, 20404–20416 (1998).
35. S. Anda, R. Zach, B. Grallert, Activation of Gcn2 in response to different stresses. *PLoS One* **12**, e0182143 (2017).
36. S. A. Wek, S. Zhu, R. C. Wek, The histidyl-tRNA synthetase-related sequence in the eIF-2 alpha protein kinase GCN2 interacts with tRNA and is required for activation in response to starvation for different amino acids. *Mol. Cell. Biol.* **15**, 4497–4506 (1995).
37. J. Dong, H. Qiu, M. Garcia-Barrio, J. Anderson, A. G. Hinnebusch, Uncharged tRNA activates GCN2 by displacing the protein kinase moiety from a bipartite tRNA-binding domain. *Mol. Cell* **6**, 269–279 (2000).
38. B. A. Castilho *et al*., Keeping the eIF2 alpha kinase Gcn2 in check. *Biochim. Biophys. Acta* **1843**, 1948–1968 (2014).
39. S. J. Lee, M. J. Swanson, E. Sattlegger, Gcn1 contacts the small ribosomal protein Rps10, which is required for full activation of the protein kinase Gcn2. *Biochem. J.* **466**, 547–559 (2015).
40. E. Sattlegger, A. G. Hinnebusch, Polyribosome binding by GCN1 is required for full activation of eukaryotic translation initiation factor 2alpha kinase GCN2 during amino acid starvation. *J. Biol. Chem.* **280**, 16514–16521 (2005).
41. C. Tian, T. Kasuga, M. S. Sachs, N. L. Glass, Transcriptional profiling of cross pathway control in *Neurospora crassa* and comparative analysis of the Gcn4 and CPC1 regulons. *Eukaryot. Cell* **6**, 1018–1029 (2007).
42. V. M. Advani, P. Ivanov, Translational control under stress: Reshaping the translatome. *BioEssays* **41**, e1900009 (2019).
43. I. B. Barthelmess, J. Kolanus, The range of amino acids whose limitation activates general amino-acid control in *Neurospora crassa*. *Genet. Res.* **55**, 7–12 (1990).
44. H. J. Flint, B. F. Kemp, General control of arginine biosynthetic enzymes in *Neurospora crassa*. *J. Gen. Microbiol.* **124**, 129–140 (1981).
45. A. G. Hinnebusch, Transcriptional and translational regulation of gene expression in the general control of amino-acid biosynthesis in *Saccharomyces cerevisiae*. *Prog. Nucleic Acid Res. Mol. Biol.* **38**, 195–240 (1990).
46. M. S. Sachs, "General and corss-pathway controls of amino acid biosynthesis" in *The Mycota: Biochemistry and Molecular Biology*, R. M. G. A. Brambl, Ed. (Spinger, Heidelberg, Germany, 1996), Vol. III, pp. 315–345.
47. A. G. Hinnebusch, Molecular mechanism of scanning and start codon selection in eukaryotes. *Microbiol. Mol. Biol. Rev.* **75**, 434–467 (2011).
48. I. P. Ivanov *et al*., Translation initiation from conserved non-AUG codons provides additional layers of regulation and coding capacity. *MBio* **8**, e00844-17 (2017).
49. K. M. Vattem, R. C. Wek, Reinitiation involving upstream ORFs regulates ATF4 mRNA translation in mammalian cells. *Proc. Natl. Acad. Sci. U.S.A.* **101**, 11269–11274 (2004).
50. M. Carsiotis, R. F. Jones, A. C. Wesseling, Cross-pathway regulation: Histidine-mediated control of histidine, tryptophan, and arginine biosynthetic enzymes in *Neurospora crassa*. *J. Bacteriol.* **119**, 893–898 (1974).
51. N. Y. Garceau, Y. Liu, J. J. Loros, J. C. Dunlap, Alternative initiation of translation and time-specific phosphorylation yield multiple forms of the essential clock protein FREQUENCY. *Cell* **89**, 469–476 (1997).
52. W. J. Belden *et al*., The band mutation in *Neurospora crassa* is a dominant allele of ras-1 implicating RAS signaling in circadian output. *Genes Dev.* **21**, 1494–1505 (2007).
53. T. M. Lamb, J. Vickery, D. Bell-Pedersen, Regulation of gene expression in *Neurospora crassa* with a copper responsive promoter. *G3 (Bethesda)* **3**, 2273–2280 (2013).
54. E. Sattlegger, A. G. Hinnebusch, Separate domains in GCN1 for binding protein kinase GCN2 and ribosomes are required for GCN2 activation in amino acid-starved cells. *EMBO J.* **19**, 6622–6633 (2000).
55. J. L. Hilton, P. C. Kearney, B. N. Ames, Mode of action of the herbicide, 3-amino-1,2,4-triazole(amitrole): Inhibition of an enzyme of histidine biosynthesis. *Arch. Biochem. Biophys.* **112**, 544–547 (1965).
56. H. Qiu, C. Hu, J. Dong, A. G. Hinnebusch, Mutations that bypass tRNA binding activate the intrinsically defective kinase domain in GCN2. *Genes Dev.* **16**, 1271–1280 (2002).
57. C. Sancar, G. Sancar, N. Ha, F. Cesbron, M. Brunner, Dawn- and dusk-phased circadian transcription rhythms coordinate anabolic and catabolic functions in *Neurospora*. *BMC Biol.* **13**, 17 (2015).
58. A. R. Kubelik, B. Turcq, A. M. Lambowitz, The *Neurospora crassa cyt-20* gene encodes cytosolic and mitochondrial valyl-tRNA synthetases and may have a second function in addition to protein synthesis. *Mol. Cell. Biol.* **11**, 4022–4035 (1991).
59. I. S. B. Larsen, Y. Narimatsu, H. Clausen, H. J. Joshi, A. Halim, Multiple distinct O-Mannosylation pathways in eukaryotes. *Curr. Opin. Struct. Biol.* **56**, 171–178 (2019).

60. D. Bell-Pedersen, M. L. Shinohara, J. J. Loros, J. C. Dunlap, Circadian clock-controlled genes isolated from *Neurospora crassa* are late night- to early morning-specific. *Proc. Natl. Acad. Sci. U.S.A.* **93**, 13096–13101 (1996).
61. T. D. Baird, R. C. Wek, Eukaryotic initiation factor 2 phosphorylation and translational control in metabolism. *Adv. Nutr.* **3**, 307–321 (2012).
62. P. D. Lu, H. P. Harding, D. Ron, Translation reinitiation at alternative open reading frames regulates gene expression in an integrated stress response. *J. Cell Biol.* **167**, 27–33 (2004).
63. S. Park *et al*., Elongation factor 2 and fragile X mental retardation protein control the dynamic translation of Arc/Arg3.1 essential for mGluR-LTD. *Neuron* **59**, 70–83 (2008).
64. D. B. Weatherill *et al*., Compartment-specific, differential regulation of eukaryotic elongation factor 2 and its kinase within *Aplysia* sensory neurons. *J. Neurochem.* **117**, 841–855 (2011).
65. Y. Liu, N. Y. Garceau, J. J. Loros, J. C. Dunlap, Thermally regulated translational control of FRQ mediates aspects of temperature responses in the *Neurospora* circadian clock. *Cell* **89**, 477–486 (1997).
66. S. Zhu, A. Y. Sobolev, R. C. Wek, Histidyl-tRNA synthetase-related sequences in GCN2 protein kinase regulate in vitro phosphorylation of eIF-2. *J. Biol. Chem.* **271**, 24989–24994 (1996).
67. J. M. K. S. Fustin, S. Karakawa, H. Okamura, Circadian profiling of amino acids in the SCN and cerebral cortex by laser capture microdissection-mass spectrometry. *J. Biol. Rhythms* **32**, 609–620 (2017).
68. S. L. Spurgeon, W. H. Matchett, Inhibition of aminoacyl-transfer ribonucleic acid synthetases and the regulation of amino acid biosynthetic enzymes in *Neurospora crassa*. *J. Bacteriol.* **129**, 1303–1312 (1977).
69. A. Crnković, O. Vargas-Rodriguez, D. Söll, Plasticity and constraints of tRNA aminoacylation define directed evolution of aminoacyl-tRNA synthetases. *Int. J. Mol. Sci.* **20**, E2294 (2019).
70. R. C. Wek, J. F. Cannon, T. E. Dever, A. G. Hinnebusch, Truncated protein phosphatase GLC7 restores translational activation of GCN4 expression in yeast mutants defective for the eIF-2 alpha kinase GCN2. *Mol. Cell. Biol.* **12**, 5700–5710 (1992).
71. V. Cherkasova, H. Qiu, A. G. Hinnebusch, Snf1 promotes phosphorylation of the α subunit of eukaryotic translation initiation factor 2 by activating Gcn2 and inhibiting phosphatases Glc7 and Sit4. *Mol. Cell. Biol.* **30**, 2862–2873 (2010).
72. R. H. Davis, F. J. de Serres, Genetic and microbiological research techniques for *Neurospora crassa*. *Methods Enzymol.* **27A**, 79–143 (1970).
73. V. D. Gooch *et al*., Fully codon-optimized luciferase uncovers novel temperature characteristics of the *Neurospora* clock. *Eukaryot. Cell* **7**, 28–37 (2008).
74. M. L. Pall, J. P. Brunelli, A series of six compact fungal transformation vectors containing polylinkers with multiple unique restriction sites. *Fungal Genet. Rep.* **40** (1993).
75. D. J. Ebbole, M. S. Sachs, A rapid and simple method for isolation of *Neurospora crassa* homokaryons using microconidia. *Fungal Genet. Newsl.* **37**, 17–18 (1990).
76. N. Bardiya, P. K. Shiu, Cyclosporin A-resistance based gene placement system for *Neurospora crassa*. *Fungal Genet. Biol.* **44**, 307–314 (2007).
77. A. K. Beasley, T. M. Lamb, W. K. Versaw, D. Bell-Pedersen, A ras-1bd Mauriceville strain for mapping mutations in Oak Ridge ras-1bd strains. *Fungal Genet. Rep.* **53**, 30–33 (2006).
78. L. F. Larrondo, J. J. Loros, J. C. Dunlap, High-resolution spatiotemporal analysis of gene expression in real time: In vivo analysis of circadian rhythms in *Neurospora crassa* using a FREQUENCY-luciferase translational reporter. *Fungal Genet. Biol.* **49**, 681–683 (2012).
79. T. M. Lamb, C. S. Goldsmith, L. Bennett, K. E. Finch, D. Bell-Pedersen, Direct transcriptional control of a p38 MAPK pathway by the circadian clock in *Neurospora crassa*. *PLoS One* **6**, e27149 (2011).
80. C. A. Jones, S. E. Greer-Phillips, K. A. Borkovich, The response regulator RRG-1 functions upstream of a mitogen-activated protein kinase pathway impacting asexual development, female fertility, osmotic stress, and fungicide resistance in *Neurospora crassa*. *Mol. Biol. Cell* **18**, 2123–2136 (2007).
81. C. A. Schneider, W. S. Rasband, K. W. Eliceiri, NIH image to imageJ: 25 years of image analysis. *Nat. Methods* **9**, 671–675 (2012).
82. H. Liu, J. H. Naismith, A simple and efficient expression and purification system using two newly constructed vectors. *Protein Expr. Purif.* **63**, 102–111 (2009).
83. T. Zielinski, A. M. Moore, E. Troup, K. J. Halliday, A. J. Millar, Strengths and limitations of period estimation methods for circadian data. *PLoS One* **9**, e96462 (2014).
84. Z. Wang, M. S. Sachs, Arginine-specific regulation mediated by the *Neurospora crassa arg-2* upstream open reading frame in a homologous, cell-free in vitro translation system. *J. Biol. Chem.* **272**, 255–261 (1997).
85. J. Jiang *et al*., Promoter demethylation of the asparagine synthetase gene is required for ATF4-dependent adaptation to asparagine depletion. *J. Biol. Chem.* **294**, 18674–18684 (2019).